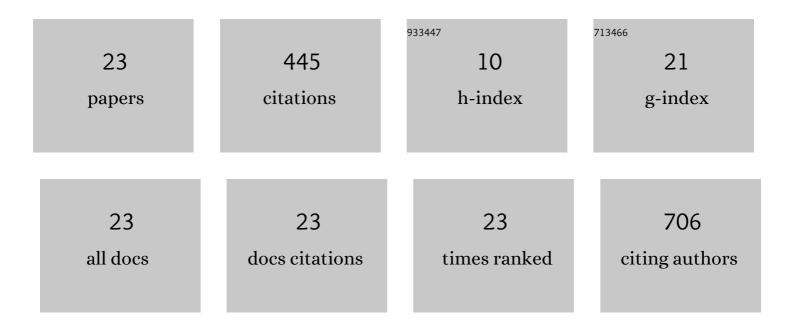
Kathryn A Morton

List of Publications by Year in descending order

Source: https://exaly.com/author-pdf/2327957/publications.pdf Version: 2024-02-01



#	Article	lF	CITATIONS
1	Bidirectional Changes in Myocardial ¹⁸ F-Fluorodeoxyglucose Uptake After Human Ventricular Unloading. Circulation, 2022, 145, 151-154.	1.6	2
2	PET-CT in Clinical Adult Oncology: III. Gastrointestinal Malignancies. Cancers, 2022, 14, 2668.	3.7	7
3	PET-CT in Clinical Adult Oncology—V. Head and Neck and Neuro Oncology. Cancers, 2022, 14, 2726.	3.7	6
4	PET-CT in Clinical Adult Oncology: II. Primary Thoracic and Breast Malignancies. Cancers, 2022, 14, 2689.	3.7	4
5	PET-CT in Clinical Adult Oncology—VI. Primary Cutaneous Cancer, Sarcomas and Neuroendocrine Tumors. Cancers, 2022, 14, 2835.	3.7	4
6	PET-CT in Clinical Adult Oncology—IV. Gynecologic and Genitourinary Malignancies. Cancers, 2022, 14, 3000.	3.7	11
7	Rapamycin restores brain vasculature, metabolism, and blood-brain barrier in an inflammaging model. GeroScience, 2021, 43, 563-578.	4.6	17
8	SPECT/CT in the Evaluation of Suspected Skeletal Pathology. Tomography, 2021, 7, 581-605.	1.8	12
9	Analysis of retention of gadolinium by brain, bone, and blood following linear gadoliniumâ€based contrast agent administration in rats with experimental sepsis. Magnetic Resonance in Medicine, 2020, 83, 1930-1939.	3.0	16
10	Prospective Evaluation of Bone Metabolic Markers as Surrogate Markers of Response to Radium-223 Therapy in Metastatic Castration-resistant Prostate Cancer. Clinical Cancer Research, 2020, 26, 2104-2110.	7.0	15
11	Anti-inflammatory agent, OKN-007, reverses long-term neuroinflammatory responses in a rat encephalopathy model as assessed by multi-parametric MRI: implications for aging-associated neuroinflammation. GeroScience, 2019, 41, 483-494.	4.6	13
12	Lipopolysaccharide exposure in a rat sepsis model results in hippocampal amyloid-β plaque and phosphorylated tau deposition and corresponding behavioral deficits. GeroScience, 2019, 41, 467-481.	4.6	28
13	Lipopolysaccharide endotoxemia induces amyloid-β and p-tau formation in the rat brain. American Journal of Nuclear Medicine and Molecular Imaging, 2018, 8, 86-99.	1.0	27
14	18 F-fluoro-2-deoxyglucose PET informs neutrophil accumulation and activation in lipopolysaccharide-induced acute lung injury. Nuclear Medicine and Biology, 2017, 48, 52-62.	0.6	24
15	Comparison of Performance of Improved Serum Estimators of Glomerular Filtration Rate (GFR) to ^{99m} Tc-DTPA GFR Methods in Patients with Hepatic Cirrhosis. Journal of Nuclear Medicine Technology, 2017, 45, 42-49.	0.8	5
16	Optimization of saturation-recovery dynamic contrast-enhanced MRI acquisition protocol: monte carlo simulation approach demonstrated with gadolinium MR renography. NMR in Biomedicine, 2016, 29, 969-977.	2.8	3
17	Performance of an efficient imageâ€registration algorithm in processing MR renography data. Journal of Magnetic Resonance Imaging, 2016, 43, 391-397.	3.4	6
18	FDG and FLT-PET for Early measurement of response to 37.5 mg daily sunitinib therapy in metastatic renal cell carcinoma. Cancer Imaging, 2015, 15, 15.	2.8	35

KATHRYN A MORTON

#	Article	IF	CITATIONS
19	Histamine Receptor 1 and 2 Antagonists Alter Biodistribution of Radioiodine. Journal of Nuclear Medicine Technology, 2015, 43, 214-219.	0.8	2
20	Comparison of 18F-Fluorodeoxyglucose and 18F-Fluorothymidine PET in Differentiating Radiation Necrosis From Recurrent Glioma. Clinical Nuclear Medicine, 2012, 37, 854-861.	1.3	61
21	Comparison of Whole-Body PET/CT, Dedicated High-Resolution Head and Neck PET/CT, and Contrast-Enhanced CT in Preoperative Staging of Clinically M0 Squamous Cell Carcinoma of the Head and Neck. Journal of Nuclear Medicine, 2009, 50, 1205-1213.	5.0	103
22	The use of computer-assisted diagnosis in cardiac-perfusion nuclear medicine studies: A review. Journal of Digital Imaging, 1992, 5, 209-222.	2.9	8
23	Gastric emptying after gastric interposition for cancer of the esophagus or hypopharynx. Annals of Thoracic Surgery, 1991, 51, 759-763.	1.3	36